EUROPEAN ORGANIZATION FOR NUCLEAR RESEARCH

CERN-EP/84-93
25 July 1984

ELASTIC SCATTERING OF ANTIPROTONS FROM CARBON, CALCIUM, AND LEAD AT 180 MeV

D. Garreta, P. Birien, G. Bruge, A. Chaumeaux, D.M. Drake[1], S. Janouin, D. Legrand, M.C. Lemaire, B. Mayer, J. Pain and J.C. Peng[1]
DPHN/ME, CEN, Saclay, France

M. Berrada, J.P. Bocquet, E. Monnand, J. Mougey and P. Perrin
DRF, CEN, Grenoble, France

E. Aslanides and O. Bing
CRN, Strasbourg, France

J. Lichtenstadt and A.I. Yavin
Tel Aviv University[2], Tel Aviv, Israel

ABSTRACT

Angular distributions for elastic scattering of 180 MeV antiprotons from ^{12}C, ^{40}Ca, and ^{208}Pb have been measured over a wide angular range with a magnetic spectrometer. In general, microscopic calculations agree fairly well with the data. Optical-model fits with Woods-Saxon parametrization determine the magnitude and the relative strength of the real and imaginary potentials at the nuclear surface. When the shape of the potentials is derived from that of the charge distribution, the depth of the real potential is found to be shallow ($30\ \text{MeV} < V_0 < 70\ \text{MeV}$). These results are in some disagreement with several models and predictions, but are consistent with the results of $\bar{p}$-^{12}C scattering at 46.8 MeV and with a recent analysis of $\bar{p}$-atom data.

(Submitted to Physics Letters B)

1. Permanent address: Los Alamos National Laboratory, New Mexico, USA. Supported in part by the US Department of Energy.
2. Supported in part by the Fund for Basic Research of the Israel Academy of Sciences.

The study of $\bar{p}$-nucleus interaction is a topic of great interest, especially since the availability of high-quality antiproton beams delivered by the Low-Energy Antiproton Ring (LEAR) [1]. Indeed the experimental data taken at other facilities are quite scarce and of rather poor quality. They consist mainly of bubble-chamber data [2], antiproton cross-sections on carbon, aluminium, and copper [3, 4], and level widths and shifts from X-ray studies of antiprotonic atoms [5]. From the analysis of these data, it was not possible to know if the real and imaginary parts of the $\bar{p}$-nucleus potential were deep or shallow, and what were their relative strengths and ranges [6, 7]. From the theoretical point of view, large ambiguities in the determination of the $\bar{p}$-nucleus potential also existed. Calculations which involve the folding of $\bar{N}N$ interaction with the matter density distribution of the nucleus led to real potentials which ranged from strongly attractive to repulsive values [7, 8]. In the relativistic mean field approach, the $\bar{p}$-nucleus potential was predicted to be strongly attractive [9]. However, in this approach, annihilation is treated phenomenologically, so that the effect of dispersive corrections on the real potential is not known.

The first high-quality elastic and inelastic angular distributions measured at LEAR by Garreta et al. [10] for the $\bar{p}$-^{12}C system at 46.8 MeV already set some constraints on the $\bar{p}$-nucleus potential. Using a Woods-Saxon geometry with reasonable values for the radius and diffuseness parameters, it was shown that the real potential is attractive but shallow ($10\ \text{MeV} < V_0 \leq 50\ \text{MeV}$), whilst the imaginary potential is about two times stronger so that orbiting [7] is not expected. Furthermore, although some ambiguity concerning the depth of the potentials in the nuclear interior still existed, the magnitude of both V and W was well determined at a distance of 3.7 fm. It was also pointed out that microscopic calculations [8, 10] with no free parameters agreed fairly well with the data. Following this measurement, the results of several theoretical calculations and analyses [11–18] have been compared with these data. By and large the conclusions concerning the optical potential at the nuclear surface were similar, and some of them [17, 18] also confirmed the good description of the data by microscopic calculations.

In the present paper we report the results of $\bar{p}$ elastic scattering from carbon, calcium, and lead at 180 MeV using the LEAR facility and the magnetic spectrometer SPES II. The main purpose of the experiment was to study how these characteristics of the $\bar{p}$-nucleus potential depend on incident energy and target mass. In contrast with recent differential cross-section measurements [4], the present data cover a much wider angular range, and the elastically scattered antiprotons are well resolved, with no pion contamination [10], so that they provide the necessary ingredients for optical-potential determination. Using microscopic calculations, they may also provide a test of the elementary $\bar{N}N$ amplitudes. Finally, it was hoped that these results, along with those at 46.8 MeV, would supply some information on the probability of $n\bar{n}$ oscillations [19].

A description of the apparatus and experimental procedure is given elsewhere [10]. Natural C, Ca, and enriched ^{208}Pb (86.5%) targets with a thickness of about 1 g/cm^2 were used. The energy resolution was about 1.2 MeV (FWHM) and the overall angular resolution, including multiple scattering in the target, varied from about 2° for the C and Ca targets to about 3° for the Pb target. The uncertainty on the absolute scattering angle was 0.2°.

The three measured angular distributions for antiprotons are shown (solid dots) in Fig. 1, which also displays the angular distributions for protons (open circles) measured at Uppsala [20]. The error bars correspond to the statistical uncertainty and to a 5% uncertainty in the solid

angle. The uncertainty on the absolute normalization is 10%. It is apparent that the angular distributions for antiprotons are diffractive, as has already been observed at 46.8 MeV; but unlike the situation at the lower energy, the magnitude of the differential cross-section in the observed angular range is larger for antiprotons than for protons.

Results of two microscopic calculations are also shown in Fig. 1. The dashed and dotted curves represent KMT-type [21] calculations done with the $\bar{p}N$ amplitudes of Dover and Richard [22] or of the Paris potential [23], respectively. The proton density was taken from electron-scattering analysis [24] and the neutron density from scattering of high-energy protons and kaons [25]. Both predictions, which have no free parameters, agree with the data reasonably well, although for ^{12}C those of Dover and Richard seem to agree better. A final decision as to which amplitudes are preferred should await the more sensitive test of inelastic scattering [11, 26]. The agreement between the experimental results and the microscopic calculations is somewhat surprising in view of the necessary conditions for KMT calculations to be valid. We note that both KMT and recent Glauber-type [27] calculations [18] also agree with the data at 46.8 MeV. A possible explanation for these agreements is that the elementary $\bar{p}N$ scattering is forward peaked, a condition favourable to multiple-scattering calculations. Our results also agree with the predictions of von Geramb et al. [17] (not shown), whose method was originally developed for nucleon - nucleus scattering with the nuclear matter approach [28]. The agreement of the prediction by Niskanen and Green [8] with the 46.8 MeV data all but disappears at 180 MeV [29]. We note that the predicted ratio V/W is very high. The disagreement could be attributed to the too early truncation of the elementary amplitude (only s and p waves) and to the use of the local t matrix at an energy which is too high [29].

Optical-model analysis of the 180 MeV data has also been performed using the ECIS code [30] with an optical potential parametrized by a Woods-Saxon geometry, with volume absorption, and with no spin orbit. Just as in the analysis of $\bar{p}$-^{12}C scattering at 46.8 MeV [10], good fits ($0.8 < \chi^2/N < 1.5$) were achieved with optical potentials having quite different geometrical parameters. Typical examples of the optical-model fits are displayed as the solid curves in fig. 1. The depth of the real part (V_0) ranged from 10 to 100 MeV, whilst the strength of the imaginary part (W_0) was always bigger. Consequently, we could again determine the magnitude of the real and imaginary potentials only at R, the radius of the strong absorption [31], whose values are displayed in table 1. We note that the optical potential is probed to a smaller distance than at 46.8 MeV and that $|W(R)| \geq 2|V(R)|$. This indicates that a necessary condition for orbiting does not exist [7, 16]. When the geometrical parameters of the real and imaginary parts are assumed to follow those of the point charge distribution, corrected for the interaction range, taken as a Yukawa function with $\mu^{-1} = 0.6$ fm, V_0 and W_0 become well determined. These values are also shown in table 1, where we can see that always $V_0 < 70$ MeV and $W_0 \geq 2V_0$. These results agree with those of the 46.8 MeV scattering data [10] and with a recent analysis [15] of $\bar{p}$ atoms, which all but removed the ambiguity [6] in the antiproton-nucleus interaction, by rejecting the shallow (S type) imaginary potentials. Moreover, the depth V_0, which for ^{12}C does not show the strong energy dependence predicted by some models [8, 9], is shallower than that calculated in the relativistic mean-field approach [9], and provides a lower limit for the $\bar{n}n$ oscillation time [19], $\tau_{\bar{n}n}$, of about 3×10^7 s. Despite the optical-model ambiguities, the reaction cross-sections are well determined in the present analysis, and their values are given in table 1. The decrease with incident energy of both R and σ_R, as seen in the table, is consistent with the energy dependence of the $\bar{p}N$

cross-section. The reaction cross-section can be represented by the expression $\sigma_R = \pi(a + r_0 A^{1/3})^2$, with $a \simeq 0.65$ fm and $r_0 \simeq 1.44$ fm. Our determination of σ_R for ^{12}C agrees with that of Nakamura et al. [4], whereas the value quoted by Aihara et al. [3] is 20% lower.

In summary, we have extended the measured information on antiproton–nucleus interaction to 180 MeV, and have again found that the real and imaginary potentials are well determined by elastic scattering only at the nuclear surface, where $|W(R)| \geq 2|V(R)|$. If we assume a Woods–Saxon geometry the real potential is found to be attractive but shallow. If the geometry is derived from that of the charge distribution, V_0 and W_0 are well determined, with $V_0 < 70$ MeV and $W_0 > 2 V_0$. These results confirm those derived from the 46.8 MeV measurement [10] and indicate that the surface of the nucleus is not transparent to antiprotons up to 180 MeV, even though 180 MeV antiprotons seem to probe the nucleus more deeply than 46.8 MeV ones. Our results do not support the orbiting idea [7, 16], the relativistic mean field approach [9], and one microscopic calculation [8, 29]; they do confirm our previous conclusions [10], as well as those of Batty et al. [15], that shallow imaginary potentials should be ruled out, and are in fair agreement with several microscopic calculations.

We would like to thank the LEAR and the South Hall Area teams for making this experiment possible. The continuous support of the technical groups of DPHNME Saclay, CEN Grenoble, and CRN Strasbourg was essential for the success of the experiment. We are grateful to B. Loiseau, J.A. Niskanen, J.M. Richard and H.-V. von Geramb for supplying us with their results prior to publication.

REFERENCES

[1] D. Garreta, Proc. Workshop on Physics at LEAR with Low-Energy Cooled Antiprotons, Erice, 1982 (eds. U. Gastaldi and R. Klapisch) (Plenum, New York, 1984), p. 533; H. Poth, ibid., p. 567; R.M. Devries and N.J. DiGiacomo, ibid., p. 543; J. Rafelski, ibid., p. 507, and S. Kahana, ibid., p. 495.

[2] L.E. Agnew et al., Phys. Rev. **108** (1957) 1545.

[3] H. Aihara et al., Nucl. Phys. **A360** (1981) 291 and references therein.

[4] K. Nakamura et al., Phys. Rev. Lett. **52** (1981) 731.

[5] C.J. Batty, Nucl. Phys. **A372** (1981) 433 and references therein.

[6] C.Y. Wong et al., Phys. Rev. **C 29** (1984) 574.
A.D. MacKellar, G.R. Satchler and C.Y. Wong, Z. Phys. **A316** (1984) 35.

[7] E.H. Auerbach et al., Phys. Rev. Lett. **46** (1981) 702.

[8] J.A. Niskanen and A.M. Green, Nucl. Phys. **A404** (1983) 495, and A.M. Green, private communication.

[9] A. Bouyssy and S. Marcos, Phys. Lett. **114B** (1982) 397, and references therein.

[10] D. Garreta et al., Phys. Lett. **135B** (1984) 266, ibid. **139B** (1984) 464.

[11] C.B. Dover et al., Antinucleon–nucleus inelastic scattering and the spin dependence of the $N\bar{N}$ annihilation potential, preprint, IPN, Orsay (1984).

[12] J. Kronenfeld, A. Gal and J.M. Eisenberg, Antiproton–nucleus scattering with self-consistent model for medium corrections, Hebrew University, Jerusalem (1984).

[13] K.I. Kubo, H. Toki and M. Igarashi, Optical potential description of antiproton–nucleus scattering at 46.8 MeV, Tokyo Metropolitan University, Tokyo (1984).

[14] T. Suzuki and H. Narumi, Hiroshima Univ. Preprint HUPD-8403 (1984).

[15] C.J. Batty, E. Friedman and J. Lichtenstadt, Optical potentials for low-energy antiproton–nucleus interactions, Rutherford Appleton Laboratory, Didcot (1984).

[16] S.H. Kahana and M.E. Sainio, Phys. Lett. **139B** (1984) 231.

[17] H.V. von Geramb, K. Nakano and L. Rikus, Microscopic analysis of antiproton scattering from carbon, Universität Hamburg, Hamburg (1984).

[18] O.D. Dalkarov and V.A. Karmanov, preprint No 77, Lebedev Inst. (1984).

[19] C.B. Dover, A. Gal and J.M. Richard, Phys. Rev. **D 27** (1983) 1090.

[20] A. Johansson et al., Ark. Fys. **19** (1961) 541.
W.T.H. Van Oers et al., Phys. Rev. **C 10** (1974) 307.

[21] A.K. Kerman, H. McManus and R.M. Thaler, Ann. Phys. **8** (1959) 551.
A. Chaumeaux et al., Ann. Phys. (NY) **116** (1978) 247.
A. Chaumeaux, Ph.D. Thesis, Université de Paris-Sud, Orsay, 1980.

[22] C.B. Dover and J.M. Richard, Phys. Rev. **C 25** (1982) 1252; and J.M. Richard, private communication.

[23] J. Coté et al., Phys. Rev. Lett. **48** (1982) 319; and B. Loiseau, private communication.

[24] I. Sick and J.S. McCarthy, Nucl. Phys. **A150** (1970) 631.
R.F. Frosch et al,, Phys. Rev. **174** (1968) 1380.
C.W. De Jager et al., Atomic Data and Nucl. Data Tables **14** (1974) 479.

[25] A. Chaumeaux and M.C. Lemaire, Phys. Rev. **C 28** (1983) 772.

[26] C.B. Dover, private communication.

[27] R.J. Glauber, Lectures in Theoretical Physics, University of Colorado, Boulder, 1958 (Interscience, NY, 1958), vol. 1, p. 315.
[28] Microscopic Optical Potentials, Hamburg, 1978 (ed. H.V. von Geramb), Lecture Notes in Physics (Springer Verlag, Berlin, 1979), vol. 89.
[29] J.A. Niskanen, private communication.
[30] J.J. Raynal, Saclay report DPM/T/72-48 (1971), unpublished.
[31] R.C. Barrett and D.F. Jackson, *in:* Nuclear sizes and structure (Clarendon Press, Oxford, 1977), 263.

Table 1

Real and imaginary potentials at the radius of the strong interaction and calculated reaction cross-sections. Also shown are the strengths of the real and imaginary potentials obtained by using a geometry derived from that of the charge distribution (see text).

Target	$E_{\bar{p}}$ (MeV)	R (fm)	V(R) (MeV)	W(R) (MeV)	σ_R (mb)	V_0 (MeV)	W_0 (MeV)
^{12}C [a)]	46.8	3.7	-3.5 ± 1.5	-8.5 ± 1	600 ± 30	35 ± 4	77 ± 4
^{12}C	179.7	3.3	-7.8 ± 1.5	-19.6 ± 2	500 ± 25	44 ± 4	96 ± 2
^{40}Ca	179.8	4.94	-6.2 ± 1.5	-13.3 ± 2	990 ± 50	43 ± 4	119 ± 3
^{208}Pb	180.3	8.15	-5.4 ± 1.5	-10.2 ± 2	2670 ± 140	60 ± 6	152 ± 2

a) Ref. [10].

Figure caption

Fig. 1 : Differential cross-sections for $\bar{p}$-elastic scattering from ^{12}C, ^{40}Ca, and ^{208}Pb (solid circles). The cross-sections for proton elastic scattering [20] are also shown for comparison (open circles). The dashed and dotted curves are KMT calculations (see text) using $\bar{N}N$ amplitudes of refs. [22] and [23], respectively. The solid curves result from an optical-model fit to the data (see text) with the following parameters: $V_0 = 30$ MeV, $r_{0v} = 1.225$ fm, and $r_{0w} = 1.1$ fm for all three targets, and $W_0 = 118$, 124, 172 MeV, $a_v = 0.514$, 0.572, 0.672 fm, and $a_w = 0.500$, 0.590, 0.649 fm for C, Ca, and Pb, respectively.

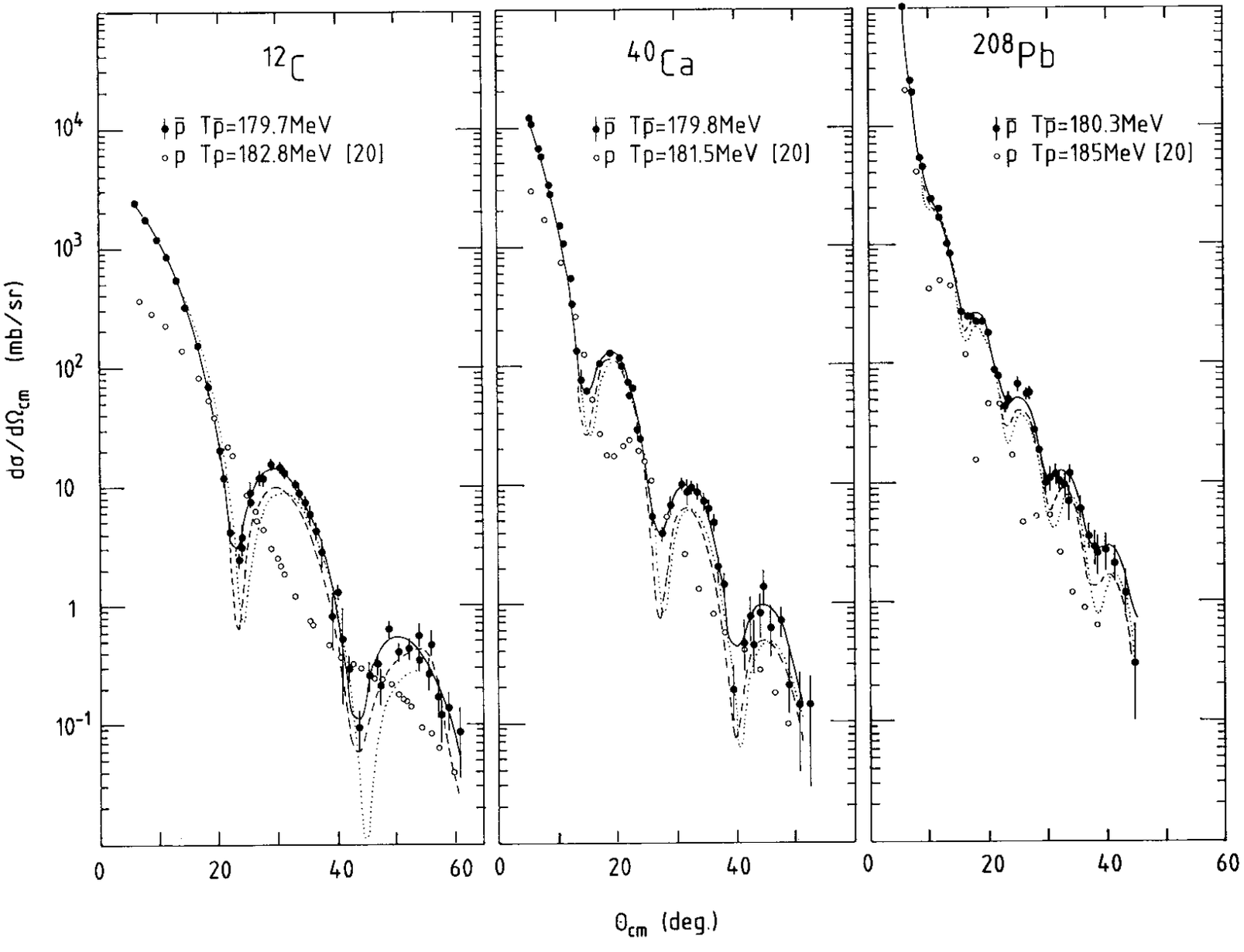
^{12}C
$\bar{p}$ $T\bar{p}$=179.7MeV
p Tp=182.8MeV [20]
^{40}Ca
$\bar{p}$ $T\bar{p}$=179.8MeV
p Tp=181.5MeV [20]
^{208}Pb
$\bar{p}$ $T\bar{p}$=180.3MeV
p Tp=185MeV [20]
$d\sigma/d\Omega_{cm}$ (mb/sr)
10^4
10^3
10^2
10
1
10^{-1}
0
20
40
60
Θ_{cm} (deg.)

Fig. 1